Vietnam Journal of Catalysis and Adsorption
Tạp chí xúc tác và hấp phụ Việt Nam

http://chemeng.hust.edu.vn/jca/

O3-type layered Ni-rich cathode: synthesis and electrochemical characterization

Nguyen Le Minh[1], Nguyen Van Hoang[1,3], Bach Le Thuy Trang[2], Tran Van Man[1,2,3], Le My Loan Phung[1,2,3,*]

[1] *Applied Physical Chemistry Laboratory (APCLAB), Faculty of Chemistry, VNUHCM-University of Science*
[2] *Department of Physical Chemistry, Faculty of Chemistry, VNUHCM-University of Science*
[3] *Vietnam National University Ho Chi Minh City, Ho Chi Minh City*
**Email: lmlphung@hcmus.edu.vn*

ARTICLE INFO

Received: 15/6/2021
Accepted: 10/7/2021
Published: 15/10/2021

Keywords:

Cathode material, diffusion coefficient, Na-ion batteries, Ni-rich, O3-type.

ABSTRACT

Ni-rich layered oxides are currently the state-of-the-art material of Lithium-ion batteries due to the balance between the cost, power and energy density. In this work, Ni-rich O3-type $Na_xNi_{0.76}Mn_{0.14}Co_{0.10}O_{2.04}$ (NMC) material was synthesized by the conventional solid-state reaction and investigated as a cathode material for sodium-ion batteries. Rietveld refinement shows that the material is high purity O3-type layered oxide of >91%. In the charge/discharge test, the material was provided the reversible capacity of 156 $mAh.g^{-1}$ initially at 0.1 C with 50% capacity retention after 50 cycles in the voltage range of 2.0 – 4.2 V. In addition, this material also demonstrates great rate-capability with the discharge capacity of 50 $mAh.g^{-1}$ even at 5 C. Therefore, NMC material could be a promising candidate for high energy sodium-ion batteries.

Introduction

Nowadays, Lithium-ion batteries (LIBs) have been widely applied in portable electronic devices and hybrid electric vehicles (HEVs). LIBs are also being considered as candidates to solve the energy demands of the transport sector owing to high energy density and power densities.[1] However, the challenges of LIBs have to regard battery safety, lifetime, poor low-temperature performance, and fabrication cost.[2] Besides, there is a great concern about the limited lithium resource and the high energy-storage cost of LIB especially when large-scale renewable energy storage has become popular.[3] Meanwhile, sodium is an abundant element, and its electropositive nature is close to lithium. Therefore, Sodium-ion batteries (SIBs) replace LIBs are inevitable with an attractive advantage in terms of cost, safety, and sustainability.[4]

Recently, O3-phase $NaTMO_2$ (TM: transition metal) materials with high capacity have been widely investigated. Comparison to P2-type material, O3-type $NaNi_xMn_yCo_zO_2$ (x + y + z =1) materials are considered to be superior because it provides higher initial charge capacity, long-term cycling performance, and better Coulombic efficiency during the charge-discharge process.[5] Various O3-type cathode materials have been explored to date such as $NaNi_{0.8}Mn_{0.1}Co_{0.1}O_2$, $NaNi_{0.6}Mn_{0.2}Co_{0.2}O_2$, $NaNi_{0.5}Mn_{0.3}Co_{0.2}O_2$ and $NaNi_{0.33}Mn_{0.33}Co_{0.33}O_2$ cathodes synthesized via co-precipitation method delivers a capacity of 187.1 $mAh.g^{-1}$, 150 $mAh.g^{-1}$, 146 $mAh.g^{-1}$, and 141 $mAh.g^{-1}$, respectively at 15 mA/g when cycled between 1.5 and 4.1 V by Hwang *et al.*[6] Sathiya and workers successfully synthesized layered $NaNi_{1/3}Mn_{1/3}Co_{1/3}O_2$ by sol-gel method, which delivers a capacity of 120 $mAh.g^{-1}$ within the voltage range

https://doi.org/10.51316/jca.2021.123

between 2 and 3.75 V.[7] Kumar et al investigated O3-phase $NaNi_{0.5}Mn_{0.3}Co_{0.2}O_2$ cathodes delivering an initial discharge capacity of ~136 $mAh.g^{-1}$ with a moderate capacity retention of 87 $mAh.g^{-1}$ at 0.1 C rate after 200 cycles.[8] The increasing percentage of the nickel > 60% in transition metal site results in an elevation of the operation voltage as well as discharge capacity, which would be basically satisfied to the demand of high energy-density batteries for electric vehicles.[9] Therefore, studying Ni-rich materials that have become attractive trends to match the future demand of SIBs for large-scale applications.

In this study, a layered O3-type Ni-rich cathode material for sodium-ion batteries was synthesized through co-precipitation followed by a solid-state reaction at 650 °C in dry air. The electrochemical properties of the Ni-rich material were evaluated. Charge/discharge performance demonstrated that the material delivered higher capacity compared to other layered oxides.

Experimental

Synthesized material preparation

$Ni_{0.76}Mn_{0.14}Co_{0.1}(OH)_2$ hydroxide precursor was synthesized by co-precipitation process according to Yujing Bi *et al.*[9] The hydroxide precursor was thoroughly mixed with NaOH at 1:1.05 molar ratio by mortar and pestle. The mixture was heated by two steps sequentially including heating at 500 °C for 10 hours and 650 °C for 20 hours in a dry airflow and both the heating rate was 5 °C/min. The sample was cooled down to 30 °C and transferred to an argon-filled glove box for storage.

Material characterization

The structure of the material was determined from X-ray diffraction (XRD) patterns collected in a D8 ADVANCED (Brucker) diffractometer using CuKα radiation (λ = 1.5814 Å) operated at a scanning rate of 0.02° per step and 1 second per step and 2θ range from 10° to 70°. Lattice parameters and percentage of phase components were calculated from XRD pattern using Rietveld refinement method. The morphology of the material and element compositions were examined using a Hitachi FE-SEM S-4800 Scanning Electron Microscope (SEM) and Energy-dispersive X-ray spectroscopy (EDS) with an accelerating voltage of 10 kV.

Electrochemical characterization

Cathode material and cell assembly were conducted in an argon-filled glovebox (GP-Campus, Jacomex, France). For the preparation of cathode electrode, the mixture consists of NMC, conducting carbon (acetylene black - C65) and poly(vinylidene fluoride-co-hexafluoropropylene) (PVDF-HFP) binder in a weight ratio of 80:15:5 was mixed by ball-milling in N-methy-2-pyrrolidone (NMP) to obtain a homogenous slurry, then it was coated on technical Al foil and dried at 100 °C for 12 hours in the antechamber of the glovebox. Then the cathode film was punched into round-shaped pieces of 12 mm diameters with the mass loading of 2-3 $mg.cm^{-2}$. Swagelok-type cell was assembled using the as-prepared cathode, a sodium slice as an anode, two Whatman filters (GF/C) as a separator, and the solution 1 M $NaClO_4$ in propylene carbonate (PC) with 2% vol fluoroethylene carbonate (FEC) additive as the electrolyte.

Electrochemical characterization was performed by a multi-channel MPG-2 and VSP battery cycler (Biologic, France). Cyclic voltammetry (CV) was recorded at the scan rate of 100 $\mu V.s^{-1}$ in the voltage range of 2.0 to 4.2 V (vs. Na^+/Na). Charge-discharge performance was evaluated at C/10 rate and at various current rates from C/10 to 2 C in the same voltage range of CV to investigate rate capability (1 C rate is current to insert/extract one sodium in 1-hour corresponding to 236.5 $mA.g^{-1}$). Electrochemical impedance spectroscopy (EIS) was obtained by applying an alternating potential signal of 10 mV in amplitude to the cell at equilibrium potential and the frequency varies from 1 MHz to 10 mHz.

Results and discussion

Crystalline structure and morphology evaluation

Figure 1 shows Rietveld refinement result of the as-prepared material. The low value of R_{wp} of 10.42 indicates the relatively good matching between the simulated pattern and the observed pattern. The pattern demonstrates that the material crystallizes in O3-type layered structure as compared to the standard (PDF No: 01-070-2030). The characterized peaks of the phase located at 2θ = 17°, 34.5°, 36.4°,

https://doi.org/10.51316/jca.2021.123

37.7°, and 42.9° corresponding diffraction from lattice planes as could be seen in the pattern. Besides, the unindexed peaks at 2θ = 37°, 43°, and 63° match the diffraction peaks of NiO, reveals that the material consists of NiO impurity along with the O3-type layered structure phase. Because of the high Ni content, the formation of NiO is unavoidable during the synthesis of Ni-rich material.[10] Rietveld refinement also indicates that the material is high purity O3-type layered oxide with relatively low NiO impurity.

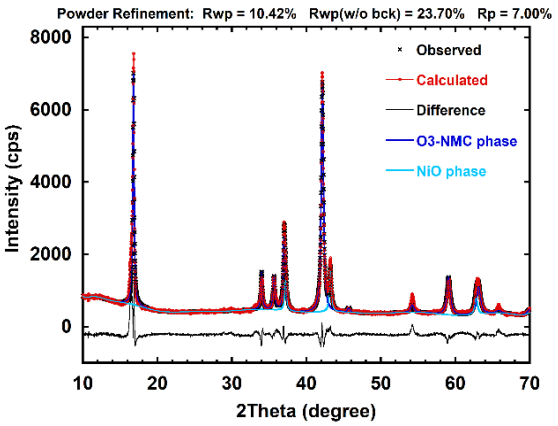

Figure 1: XRD patterns and Rietveld refinement results of NMC material

Lattice parameters and percentage of each phase present in Table 1.

Table 1: The lattice parameters calculated by Rietveld refinement

	Lattice dimensions (Å)	Volume (Å^3)	Weight percentage (%)
O3-phase	a = b = 2.949 c = 15.841	119.29	91.1
NiO	a = b = c = 4.190	73.30	8.9

SEM images of the synthesized material are presented in Figure 2(a). The material exhibits a flaky particle morphology which consists of irregular sub-micron particles. Fig 2(b) was presented EDS spectrum showing the presence of various elements in the sample. The chemical composition of the as-prepared NMC is $Na_{0.81}Ni_{0.76}Mn_{0.14}Co_{0.10}O_{2.04}$ as calculated by EDS result that consistent with the ratio of the precursors.

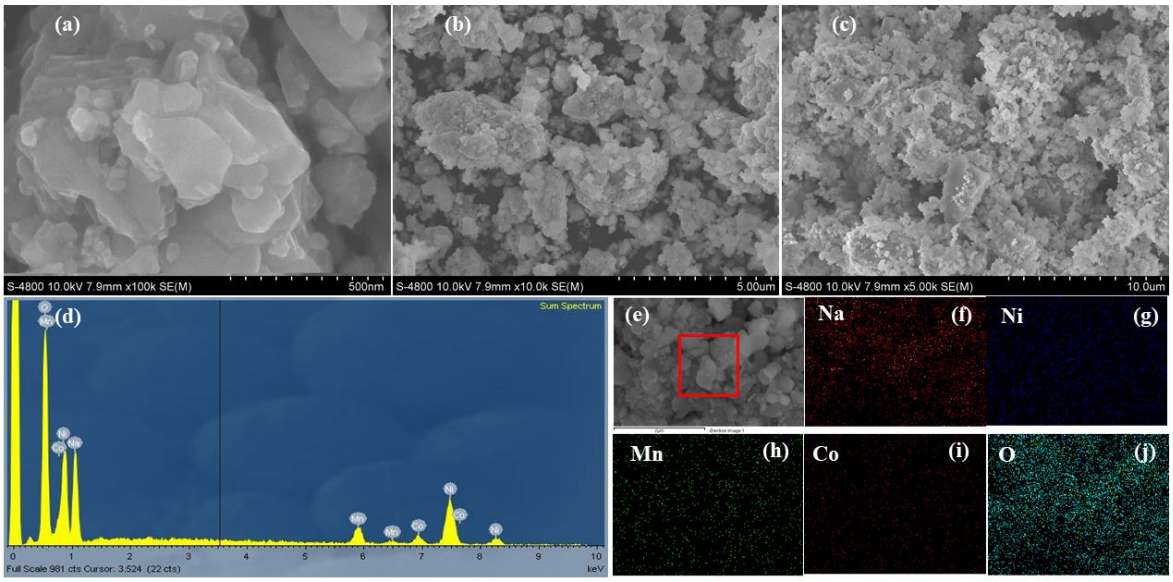

Figure 2: SEM images of the sample (a-c) and EDS spectrum showing the composition of various elements in the sample (d). SEM image and EDX analysis region (e). EDX mapping of elements (f-j)

Electrochemical properties

The electrochemical behavior and structural evolution of the NMC studied by CV presented in Fig 3. The CV shows many sharp peaks indicating successive bi-phase transitions during sodium ion intercalation during the voltage range of 1.5-4.2 V. Typically, the redox couple Mn^{4+}/Mn^{3+} is active at a low voltage of 1.5 - 2.7 V vs. Na/Na^+ [11] but inactive in Ni-rich layered oxides because all manganese atoms are at oxidation state +4.[12]

https://doi.org/10.51316/jca.2021.123

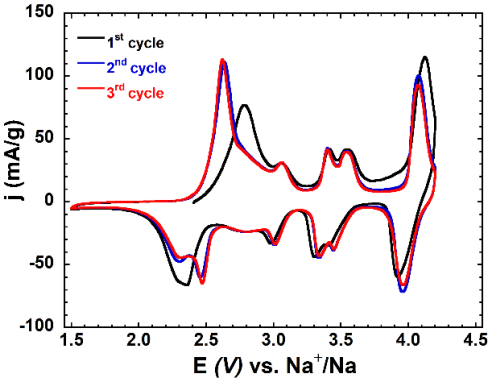

Figure 3: Cycling voltammogram of NMC material in the voltage windows: 1.5 – 4.2 V at the scan rate 100 $\mu V.s^{-1}$.

Thus, the electrochemical performance of the NMC was contributed form Ni^{3+}/Ni^{4+} and Ni^{2+}/Ni^{3+} redox couples occurs at high voltage region and low voltage region respectively.[13] Additionally, redox couple Co^{4+}/Co^{3+} probably active at above 4 V.[14] The accordance of CV feature of the material with one of previous reported [5] demonstrates that NiO impurity is inactive.

The electrochemical performance of NMC presented in Fig 4(a-b). The well-defined redox behavior of the material is also demonstrated in the charge/discharge profile with several plateaus corresponding to redox peak pairs on CV curves. These voltage plateaus reveals various phase transformations of O3–O1–P3 occurring along with MO_2 slab gliding.[14] The material shows the initial charge and discharge capacity of 260.3 and 156.5 $mAh.g^{-1}$, respectively. Thus, the Coulombic efficiency only reaches 60% at the first cycle but it increases to over 90% in the next following cycles. Although the higher capacity was obtained with higher Ni content by trigger the $Ni^{3+/4+}$ redox couple, the capacity retention was about 50% after 50 cycles. The degradation of performance of Ni-rich material that Ni content >60% have been obstacle and need to further improve. The inferior performance relate to the unstable of structure as results of slab gliding [13–15] and fast electrolyte decomposition [5,16] specially at high voltage region.

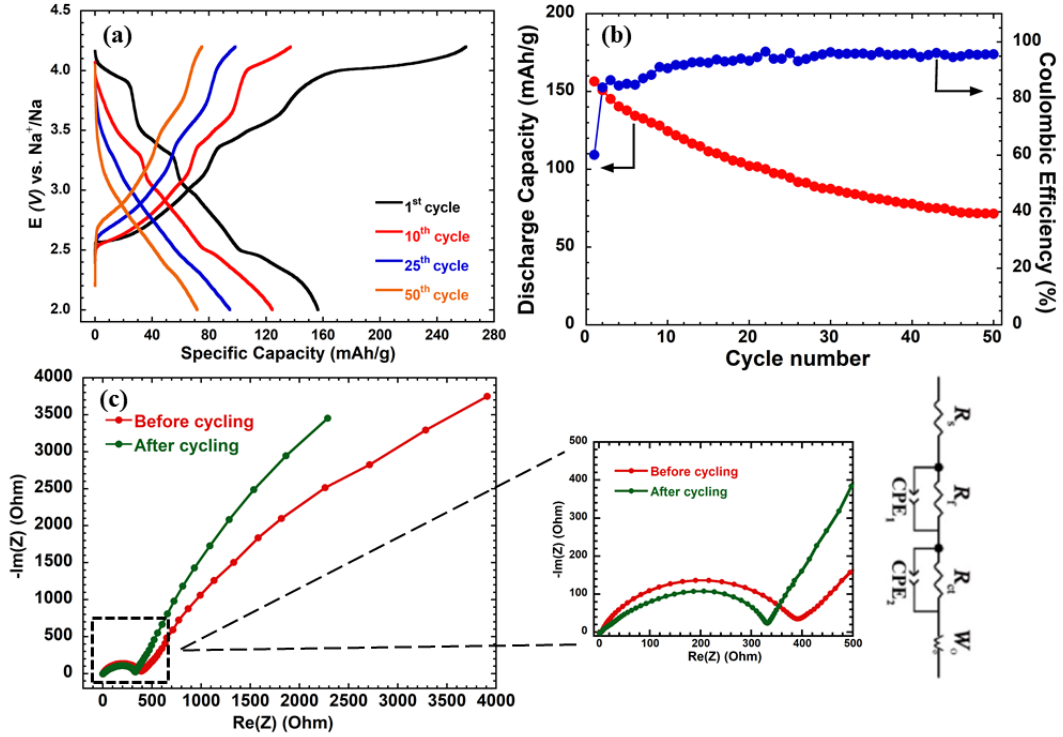

Figure 4: Charge-discharge curves (a) and cycling performance with Coulombic efficiency (b) in the voltage windows: 2.0 – 4.2 V of the NMC. EIS spectra of the NMC electrode at the before and after charge/discharge testing (c)

https://doi.org/10.51316/jca.2021.123

EIS measured before and after charge/discharge testing is showed in Fig 4(c). The Nyquist plots consist of a high-frequency semi-circle and an inclined straight line in the low-frequency region indicating the charge transfer resistance at the electrode/electrolyte interface and the migration of Na^+ in the structure respectively. Model fitting was performed using the equilavent circuit present in the same figure. As the results, the electrolyte resistance (R_s) and charge transfer resistance (R_{ct}) increases with cycling.

The electrolyte resistance before and after cycling don't change and equal to 5 Ω. The charge transfer resistance before and after cycling are 392.2 and 331.6 Ω, respectively. The decrease in R_{ct} after cycling is attributed to the increased permeability of the interface after repetitive ion intercalation/deintercalation and probaly the increase of contact area as results of structure/particle degradation.

Diffusion coefficients of sodium-ion

Figure 5(a) illustrates the CV curves of NMC electrode scanned at the rates increase gradually from 10 $\mu V.s^{-1}$ to 100 $\mu V.s^{-1}$ which presents the featured relationship between current and the scan rate in reversible manner. Therefore, the Randles-Sevcik equation is used to calculate the diffusion coefficient of sodium ion [17]:

$$I_p = (2.69\times10^5)n^{2/3}AC_oD_{Na}^{1/2}v^{1/2} \quad (1)$$

Where I_p is the peak current (A), n is the number of electron exchange, A is the geometric area of the electrode (1.13 cm^2), D_{Na} is Na^+ ion diffusion coefficient, C_o is the initial concentration of ion Na^+ in the unit cell. C_o is calculated from the molar of sodium ion in the unit cell and volume of the unit cell.

The calculated value of D_{Na} are comparable with literature results for layered oxides.[7,13,14] The D_{Na} change from 1.90×10^{-12} to 1.16×10^{-11} and from 1.58×10^{-12} to 3.55×10^{-12} on charge and discharge respectively (Fig 5(b)). The values tend to strongly decrease in the first pair of peaks and then gradually increase in the other peak pairs in both charge and discharge. As mentioned, the NMC displays the phase transformations of O3–O1–P3 along with MO_2 slab gliding during sodiation/desodiation,[12,14] in accordance with the change of D_{Na} and the reduce of D_{Na} in bi-phasic region that detrimental to the migration of sodium ion in the structure.

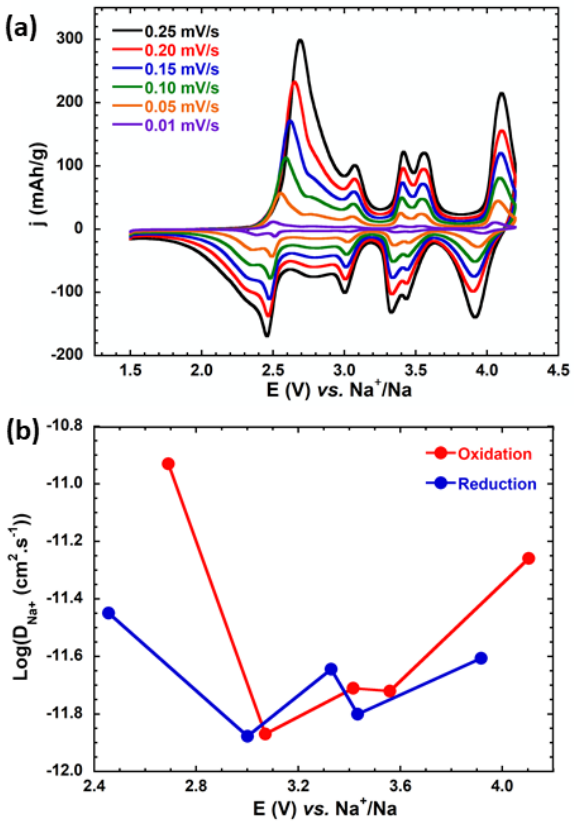

Figure 5: Cyclic voltammogram recorded at various scan rates of NMC (a) and the plot of diffusion coefficients calculated at an oxidation/reduction peak of the sample in the CV curves (b)

Conclusion

O3-type Ni-rich cathode material $Na_{0.81}Ni_{0.76}Mn_{0.14}Co_{0.10}O_{2.04}$ was prepared by the conventional solid-state reaction with a minor NiO impurity. The as-prepared NMC material not only shows typical electrochemical properties that is not affected by the present of the impurity but also delivers high capacity of 156 $mAh.g^{-1}$ initially and maintain 50% its capacity after 50 cycles. Besides, the material provides a capacity of about 50 $mAh.g^{-1}$ at high rate of 5 C. The diffusion coefficient of sodium-ion (D_{Na}) calculated from the Randles-Sevcik equation is in the order of 10^{-11} - 10^{-12} $cm^2.s^{-1}$ in the oxidation and reduction process, suggesting good reversible phase transition. These results show that the Ni-rich layer oxide is a promising cathode material for high-energy density applications in the future. However, further searches are needed to overcome structure degradation that destroy the cycling stability of the material.

https://doi.org/10.51316/jca.2021.123

Acknowledgments

This research is funded by Viet Nam National University Ho Chi Minh City (VNU-HCM) under grant code B2020-18-06.

References

1. D. Larcher, J. -M. Tarascon, Nat. Chem. 7 (2015) 19–29. https://doi.org/10.1038/nchem.2085
2. H. Pan, Y. -S. Hu, L. Chen, Energy Environ. Sci. 6 (2013) 2338–2360. https://doi.org/10.1039/C3EE40847G
3. S. Y. Hong, Y. Kim, Y. Park, A. Choi, N. -S. Choi, K. T. Lee, Energy Environ. Sci. 6 (2013) 2067–2081. https://doi.org/10.1039/C3EE40811F
4. P. Vassilaras, X. Ma, X. Li, G. Ceder, J. Electrochem. Soc. 160 (2012) A207. https://doi.org/10.1149/2.023302jes
5. J. -Y. Hwang, C. S. Yoon, I. Belharouak, Y. -K. Sun, J. Mater. Chem. A 4 (2016) 17952–17959. https://doi.org/10.1039/C6TA07392A
6. M. Sathiya, K. Hemalatha, K. Ramesha, J. -M. Tarascon, A. S. Prakash, Chem. Mater. 24 (2012) 1846–1853. https://doi.org/10.1021/cm300466b
7. V. K. Kumar, S. Ghosh, S. Biswas, S. K. Martha, J. Electrochem. Soc. 167 (2020 80531. https://doi.org/10.1149/1945-7111/ab8ed5
8. J. -M. Tarascon, M. Armand. Nature 414 (2011) 171–179. https://doi.org/10.1038/35104644
9. Y. Bi, J. Tao, Y. Xu, Y. Qi, J. Xiao, Science 370 (2020) 1313–1318. https://doi.org/10.1126/science.abc3167
10. Y. Chen, S. Wang, Y. Jie, Z. Lei, R. Cao, S. Jiao, Chem. Res. Chinese Univ. 37 (2021) 280–285. https://doi.org/10.1007/s40242-021-0441-y
11. D. Yuan, X. Hu, R. Mao, X. Ai, H. Yang, Y. Cao, Electrochim. Acta 116 (2014) 300–305. https://doi.org/10.1016/j.electacta.2013.10.211
12. K. Wang, Z. -G. Wu, X. -D. Guo, B. -B. Xu, B. -H. Zhong, Electrochim. Acta 216 (2016) 51–57. https://doi.org/10.1016/j.electacta.2016.09.003
13. Y. Wang, G. Hu, X. Qi, Z. Luo, K. Du, J. Power Sources 396 (2018) 639–647. https://doi.org/10.1016/j.jpowsour.2018.06.058
14. 1Y. You, S. O. Kim, A. Manthiram, Adv. Energy Mater. 7 (2017) 1601698. https://doi.org/10.1002/aenm.201601698
15. J. Deng, W. Luo, H. Liu, H. Zhou, S. Dou, Adv. Energy Mater. 8 (2018) 1701610. https://doi.org/10.1002/aenm.201701610
16. K. Park, B. -C. Yu, J. B. Goodenough., Chem. Mater. 27 (2015) 6682–6688. https://doi.org/10.1021/acs.chemmater.5b02684
17. P. -F. Wang, Y. You, Y. -X. Yin, Y. -G. Guo, J. Mater. Chem. A 4 (2016) 17660–17664. https://doi.org/10.1039/C6TA07589D